Journal of Colloid and Interface Science 529 (2018) 180–186

Contents lists available at ScienceDirect

Journal of Colloid and Interface Science

journal homepage: www.elsevier.com/locate/jcis

Cationic polyacrylamide induced nanoparticles assembly in a cellulose nanofiber network

Vikram Singh Raghuwanshi [a,*], Uthpala Manavi Garusinghe [a], Praveena Raj [a], Nigel Kirby [b], Armin Hoell [c], Warren Batchelor [a], Gil Garnier [a,*]

[a] Bioresource Processing Research Institute of Australia (BioPRIA), Department of Chemical Engineering, Monash University, Clayton, Victoria 3800, Australia
[b] Australian Synchrotron, 800 Blackburn Rd., Clayton, Victoria 3168, Australia
[c] Helmholtz-Zentrum Berlin für Materialien und Energie, Hahn-Meitner-Platz 1, D-14109 Berlin, Germany

GRAPHICAL ABSTRACT

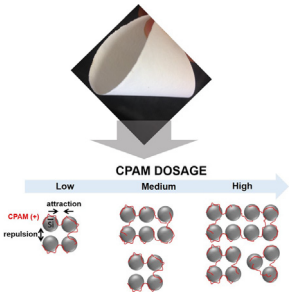

ARTICLE INFO

Article history:
Received 30 April 2018
Revised 1 June 2018
Accepted 4 June 2018
Available online 5 June 2018

Keywords:
Assembly
Silica (SiO_2)
Nanoparticles
Cationic polyacrylamide (CPAM)
Cellulose
Small Angle X-ray Scattering (SAXS)
Dynamic Light Scattering (DLS)
Scanning Electron Microscopy (SEM)

ABSTRACT

Polyacrylamides of different molecular weight, charges and dosages allow to control the retention and distribution of nanoparticles (NPs) in composites, and optimise composite properties and functionality. Our aim is to evaluate the effect of high molecular weight (13 MDa) cationic polyacrylamide (CPAM) charge and dosage on SiO_2 (74 nm) NP's assembly in cellulose nanofibers composites.

Engineered cellulose/SiO_2 composites were investigated by SEM, SAXS and DLS. SEM images show the local area retention of NPs into the cellulose matrix. SAXS provides an average NPs distribution and inter-NPs distance over complete volume of composite. DLS gives the hydrodynamic radius of CPAM adsorbed onto SiO_2 NPs in a suspension.

SAXS analysis reveals a structure conformation made of spherical SiO_2 NPs core of diameter 74 nm surrounded by a CPAM polyelectrolyte shell 2.5 nm thick. Surprisingly, CPAM induced assembly of SiO_2 NPs with constant inter-nanoparticle distance, which is irrelevant of polymer charge density. However, NPs retention in the cellulose fibre network increases with CPAM dosage. The assembly mechanism is governed by the balance of electrostatic and steric forces following CPAM coverage onto NPs and the inter-nanoparticle CPAM bridging conformation. This maintains the constant inter-nanoparticle distance and the assembly of NPs in the cellulose network.

1. Introduction

Progress in nanocellulose and nanoparticle (NP) technologies has been very fertile in the last decade, with applications lagging

* Corresponding authors.
E-mail addresses: vikram.raghuwanshi@monash.edu (V.S. Raghuwanshi), gil.garnier@monash.edu (G. Garnier).

https://doi.org/10.1016/j.jcis.2018.06.009
0021-9797/

science. Composites of nanocellulose fibrils or crystals are strong, flexible, transparent to translucent and possess low gas permeability [1,2]. However, they have poor moisture resistance and limited optical, thermal and electrical properties. Functional NPs such as metals and oxides can be incorporated into the nanocellulose fibrous network to engineer composites with novel properties [3]. NP loading up to 80 wt% and controlled NP assembling morphology have been reported using ultra high molecular weight polyelectrolytes [4]. Composites varying in structure and properties can be achieved by controlling the polyelectrolyte molecular weight, charge density and surface coverage onto NP [5].

Despite numerous theoretical [6–8] and experimental [9–12] studies, much less attention has arisen from the recent progress in ultrahigh molecular weight polyelectrolytes (over 10 MDa) [13,14]. These polymers can remain water soluble and are available from a variety of monomers and at various charge densities. High molecular weight polyelectrolytes can have a radius of gyration in the same length scale as the NP diameter with end-to end distances orders of magnitude higher, allowing many unique structures to be engineered [15].

Cationic polyacrylamide (CPAM) is a high molecular weight polyelectrolyte widely used in industry (Mw up to13 MDa). CPAM is common in papermaking as a retention aid to adhere fines, NPs and mineral fillers onto fibres [11,16]. CPAM/SiO_2 based cellulose composites combine properties of both organics, with CPAM and cellulose providing flexibility and ductility, to those of inorganics, with SiO_2 having large surface area, thermal stability, and rigidity [17]. These composites deliver high mechanical strength, dielectric, optical and barrier properties and present attractive avenues for applications in packaging, water filtration and coatings [18]. The functionality of such composites depends on the NP distribution, the interparticle interactions and their assembly within the cellulose network.

CPAM dosage significantly affects the properties and functionality of composites [20,22]. A high CPAM dosage causes NP aggregation which increases particle size but hinders the even distribution of NPs and their ability to fill the smaller pores and voids of cellulose nanofibers networks. Large NP aggregates affect the nanocomposite properties in packaging and water filtration. A low CPAM dosage results in lower NP retention in the cellulose nanofiber matrix which reduces the SiO_2 NPs contribution [19]. CPAM charge density also plays a crucial role in surface charge neutralisation, affecting the electrostatic repulsion between charged particles and their aggregates [4,20]. High charge density CPAM can lead to large NP aggregates in the cellulose network.

Previously, Salmi et al. studied layer structures formed by SiO_2 NPs and cellulose nanofibers with CPAM on a cellulose surface using QCM-D and AFM [21]. They demonstrated the SiO_2 NP's ability to penetrate into CPAM chains. However, the cellulose fibres formed individual layers between CPAM. Garnier et al. quantified the effect of CPAM charge density, concentration, and molecular weight on the aggregation of gold NPs on CPAM treated cellulose sheets. They observed an order of magnitude enhancement in the surface-enhanced Raman signals (SERS) for CPAM pre-treated sheets compared to the untreated surface [22,23]. Wagberg et al. investigated the effect of ionic strength on the adsorption of CPAM and SiO_2 NPs on silica interface by ellipsometer [24]. They reported the CPAM treated surface adsorbs high amounts of SiO_2 NPs and forms thick films; the adsorption of both CPAM and SiO_2 increases with ionic strength.

Thus, nanoparticle retention, aggregation and distribution in cellulose networks can be controlled by optimising the CPAM charge density and dosage. Still, the role of CPAM polyelectrolytes in the NPs assembly and distribution in nanocellulose structures remains poorly characterized and understood. Few techniques are available to measure the conformation of CPAM on NPs and the NP aggregate structure. This has been limiting the development of functional nanocellulose composites.

The objectives of this study are twofold. First to develop a robust analytical methodology to characterize the effect of CPAM in nanocellulose-NP composites; second, to quantify the effect of CPAM dosage and charge density on the NPs assembly formation, distribution and retention in cellulose networks. We explore methods to quantify the thickness of adsorbed CPAM layer at the NP interface and its effect on NP assemblies in cellulose composites.

Nanocomposite structure characterization was achieved by combining Small Angle X-ray Scattering (SAXS) [25,26], Dynamic Light Scattering (DLS) and Scanning Electron Microscopy (SEM) analysis. SEM provides real space images of nanostructures in cellulose network. SEM is however restricted to small surface areas and the sample preparation can produce artefacts which distort structure analysis. Alternatively, scattering methods such as DLS and SAXS are indirect non-destructive methods providing nano and microscale structure information from a larger volume. Composite structural information is extracted by fitting scattering curves with different structure models; this requires some pre-knowledge of the nanostructure morphology expected. Combining both microscopy and scattering methodologies provides a complete picture of NP assembly, distribution and their interactions within a matrix.

In this article, we are reporting the effect of CPAM dosage (surface coverage) and charge density on the assembly of SiO_2 NPs in a cellulose nanofiber network. The model NPs selected are SiO_2 of diameter 74 nm having a specific surface area of 55 m^2/g. Since both cellulose nanofibers and SiO_2 NPs are sufficiently negatively charged to form an electrostatic stabilized suspension, CPAM is used as NPs retention aid. CPAMs of different charges (10, 20, 30, 40 and 50% charge content) but constant molecular weight (13 MDa) were tested at different dosages for retaining NPs. Finally, cellulose/SiO_2 NP composite sheets were prepared by controlling the CPAM dosage and charge density. The formation and dispersion of SiO_2 NP assemblies into cellulose fibrous networks and their interactions were investigated by SAXS, SEM and DLS methods. Quantifying the influence of CPAM dosage and charge density on the NPs distributions in a cellulose network is crucial to engineer - at the nano and micro scales -the structure of cellulose/NP composites for packaging, filtration and advanced applications.

2. Experiments

2.1. Materials

Mircofibrillated cellulose (MFC) of mean diameter 73 nm and aspect ratio of 100–150 at 25 wt% solids was purchased from DAICEL Company, Japan. The cationic polyacrylamide (CPAM) polymer of molecular weight of 13 MDa and cationic charge content between 10 and 50% were kindy provided by Aquatech, Switzerland (SnowFlake series). The measured CPAM charge densities are given in Table 1. The error range in the CPAM charge density measurement is between 5 and 10%. Silicon dioxide (SiO_2)

Table 1
Measured cationic polyacrylamide (CPAM) charge densities.

CPAM charge density (wt%) from company	Charge density ($\times 10^{-3}$eq/g) measured
50	1.30
40	1.00
30	0.77
20	0.50
10	0.30

nanoparticles (at 40 wt% solids) of average diameter of 74 nm was purchased from Sigma Aldrich.

2.2. SiO_2/cellulose composite preparation

SiO_2/cellulose composite sheets were prepared by first mixing SiO_2 NPs (25 wt% of the total composite at 0.1 wt%) with the required amount of CPAM in a beaker using two peristaltic pumps. SiO_2/cellulose composites made at a fixed CPAM dosage (0.1, 0.5 or 1.0 mg CPAM/m^2 dosage) for a series of CPAM varing in charge densities (20%, 30% and 40%). The SiO_2/CPAM suspension was similarly mixed with the 1.2 g MFC/water suspension using two peristaltic pumps to the final composite suspension. Each step had a mixing time of 8 min. Final composites sheets were obtained by pouring the final suspension in a British handsheet maker with a woven filter; the wet webs were dried at 105 °C in a sheet drier.

2.3. Scanning Electron Microscopy (SEM)

Scanning electron micrographs (SEM) of the composite sheets were made on a FEI Magellan 400 FEGSEM. Samples were cut into 3×3 mm^2 samples mounted onto a metal sample holder and coated with a thin layer of Iridium prior to imaging.

2.4. Small Angle X-ray Scattering (SAXS)

SAXS measurements of the composite sheets were performed at the SAXS/WAXS beamline of the Australian Synchrotron, Australia [27]. SAXS measurements were made at an energy of 12 keV (λ = 1.033 Å) at 2 sample to detector distances (7 m and 1 m) covering the q range between ~0.001 and 0.2 $Å^{-1}$. The scattered photons from the sample were collected using a PILATUS 1 M detector (pixel size 172 μm × 172 μm). Silver behenate was used to calibrate the q scale. Scattering curves were normalized to an absolute scattering cross section by the pre-calibrated scattering curve of the glassy carbon. Final scattering curves were extracted after the data reduction and radial averaging using the beamline specific ScatterBrain software.

2.5. Dynamic Light Scattering (DLS)

A fresh 0.1 mg/mL of CPAM solution was prepared at least 8 h prior to the experiment. SiO_2 NPs were diluted to 0.5 wt% from the stock solution. The SiO_2 NPs and CPAM solution was sonicated for 2 min at 100% amplitude, respectively, to ensure evenly distribution. SiO_2 NPs suspension was then added through a peristaltic pump at 10 mL/min into the CPAM solution which was stirred at 200 rpm/min with a magnetic stirrer. This method of addition allowed the SiO_2 NPs suspension to be added drop by drop into the CPAM solution. This process was repeated for different surface coverages of CPAM to nanoparticle. Dynamic Light Scattering (DLS) using a Nanobrook Omni (Brookhaven) instrument was used to measure the hydrodynamic size of the NPs with adsorbed CPAM layers.

3. Results

The thin SiO_2/cellulose composite sheets (Fig. 1a) were first characterized by SEM to visualise the retention and structure formed by the SiO_2 NPs in the cellulose fibre network. Fig. 1b shows the SEM micrograph of SiO_2 NPs retained in the presence of CPAM. Complementary SEM images are provided in supporting information (S1). The micrograph illustrates NPs achieve high retention by assembling to fill the interfiber gaps of the cellulose fibre network; very few isolated NP are observed. However, SEM provides punctual information over a localised area and provides limited statistical data on structure, CPAM conformations, NP interface, inter NPs distances and interactions over a significant volume. Energy dispersive spectroscopy (EDS) shows the distribution of carbon, oxygen and silicon of SiO_2 – nano cellulose composites (supporting information, S2).

Small Angle X-ray Scattering (SAXS) is a well recognised non-destructive method to charaterize nanostructures (1–1000 nm) over a complete volume [28]. All SAXS experiments were performed under high flux mode at the Australian synchrotron facility. Fig. 2 shows the SAXS curves for the composites made of SiO_2 NPs dispersed into a cellulose fibre network and prepared using CPAM of different charge density (20%, 30%, 40%) and dosage (0.1, 0.5 and 1 mg CPAM/m^2). These dosage were selected to correspond roughly to minor, half and full polymer surface coverage on NPs.

All SAXS curves show the same shape with mutiple peaks and intensity varying for the composites made at different CPAM dosages. The mutiple peaks of the curves indicate assemblies of SiO_2 NPs having a fixed inter NPs distance in the cellulose fibre network.

Fig. 2(a1, b1, c1) shows the SAXS curves for SiO_2/cellulose composites made at a fixed CPAM dosage (0.1, 0.5 or 1.0 mg CPAM/m^2 dosage) for a series of CPAM varing in charge densities (20%, 30% and 40%). At a fixed CPAM dosage, varying CPAM charge density has no effect on the SAXS curves shape and intensity profile; SAXS curves are all identical.

Fig. 2(a2, b2, c2) displays the SAXS curves for SiO_2/cellulose composites at a fixed CPAM charge density but with CPAM dosages varying from 0.1 to 1 mg CPAM/m^2. At a given CPAM charge density, varying the CPAM dosage does not change the SAXS curves shape and only increases the scattering intensity with CPAM dosage. An increase in the SAXS scattering curves indicates an increase in the retention of NPs in the cellulose matrix.

Further information from the SAXS curves was extracted by fitting with a form factor including a distribution function. SiO_2 NPs are interacting with each other, forming the assemblies in cellulose fibrous network visible by SEM; a structure factor is therefore included in the fitting procedure. A log normal distribution with spherical core shell model form factor and a hard sphere structure factor fits well the scattering curves [19,29].

SAXS data fitting and analysis reveals the formation of a spherical core shell structure with a SiO_2 core of diameter 75 nm surrounded by a thin CPAM shell of 2.5 nm thickness. The relative electron density profile evaluated in Fig. 3a indicates that the SiO_2 core has a higher electron density while the CPAM shell has a lower electron density than the cellulose matrix. This is in agreement with the trend in the mass density of SiO_2 (2.5 g/cm^3), the CPAM shell 1.1 g/cm^3 and cellulose 1.5 g/cm^3.

The structure factor profiles obtained from fitting the SAXS curves of the composites with 30% CPAM charge density and at different CPAM dosages are shown in Fig. 3b. Structure factor profile shows multiple peaks for each sample. However, there are no changes in the structure factor profile observed as increases the CPAM dosage. Similarly, the structure factor at a given CPAM dosage for polymers of different charge density does not change. Multiple structure factor peaks with no change indicate the formation of NPs assemblies having a constant inter NPs distance.

SAXS analysis of solid composite sheets provides key information on the formation of the CPAM layer over SiO_2 NPs and the inter NPs interactions in the cellulose network. However, to probe only the CPAM-SiO_2 NPs interactions, Dynamic Light Scattering (DLS) is a unique technique. Experiments were performed at low SiO_2 NPs concentration at different CPAM charge density and dosages. DLS is sensitive at the higher concentrations and provides unreliable

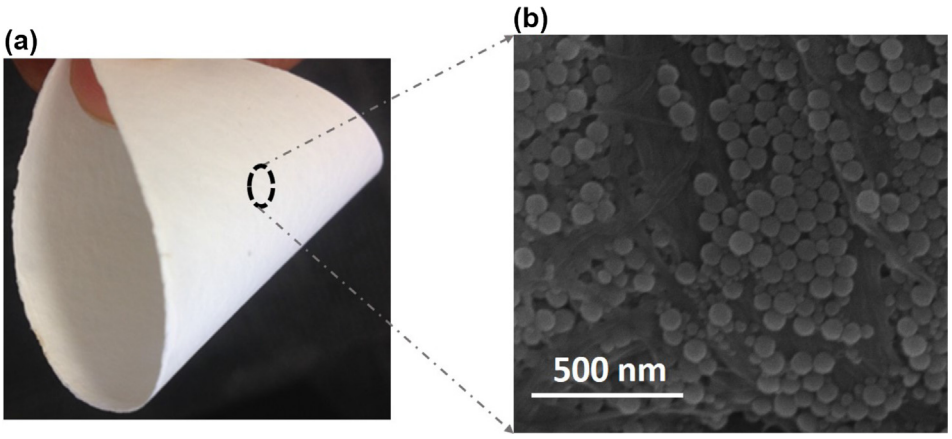

Fig. 1. (a) Picture of the thin and flexible SiO_2/Cellulose composite. (b) SEM micrographs showing retention and distribution of 74 nm SiO_2 NPs in the cellulose fibre network.

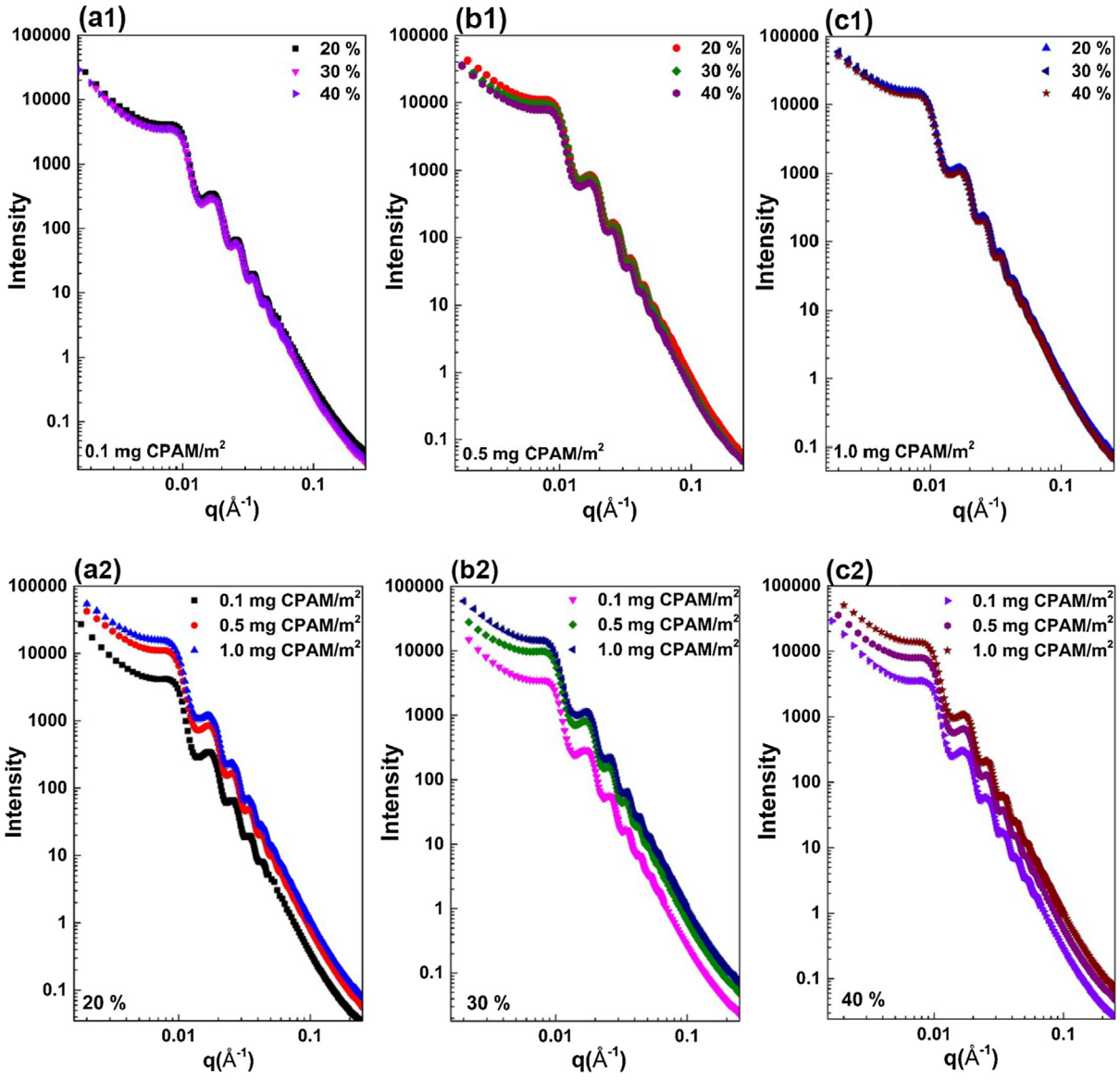

Fig. 2. SAXS curves for the SiO_2/cellulose composites with different CPAM charge density and dosages. SAXS curves for varying CPAM charge density 20, 30 and 40% at a constant CPAM dosage of 0.1, 0.5 and 1.0 mg CPAM/m^2 are given in a1, b1 and c1, respectively. SAXS curves for varying CPAM dosages 0.1, 0.5 and 1.0 mg CPAM/m^2 at a constant CPAM charge density of between 20%, 30% and 40% are given in a2, b2 and c2, respectively.

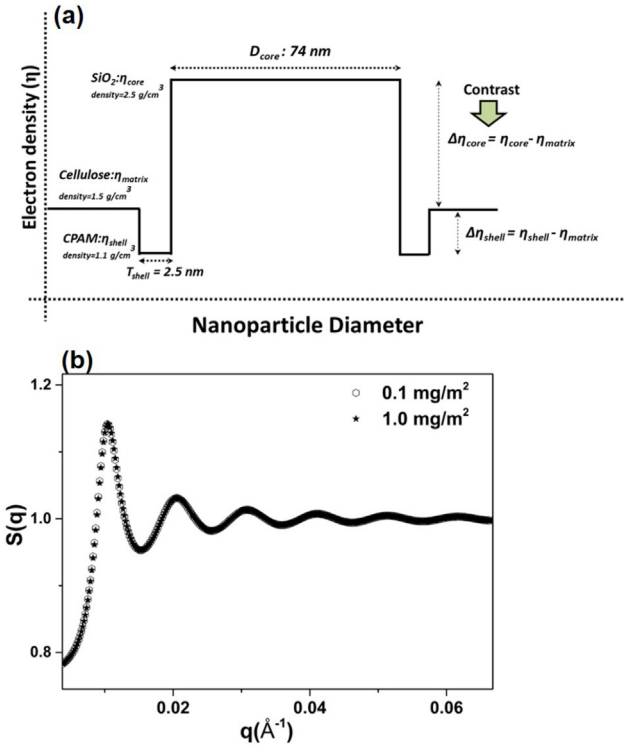

Fig. 3. (a) Relative electron density distribution obtained from SAXS curve fitting. (b) Hard sphere structure factor obtained from fitting the SAXS curves in Fig. 2(b2).

results; therefore, low concentrations of SiO_2 NPs were used. DLS measurements provides the hydrodynamic size of the particle characterized by the Brownian motion of NPs in suspension [30].

Fig. 4 shows the DLS correlation curves and lognormal size distributions of SiO_2 NPs with CPAM dosages of 0.1 and 1.0 mg CPAM/m^2, and for CPAM charge density of 10%, 30% and 50%. The correlation curves for dosage of 0.1 mg CPAM/m^2 at different CPAM charge density decays at the same rate (Fig. 4a1) and their size distributions are nearly identical (Fig. 4a2). The correlation curves for 1.0 mg CPAM/m^2 dosage in Fig. 4b1 shows a faster decay for 10% charge density and a slower decay for 30% and 50%. The average lognormal mean hydrodynamic diameter is large for 50% charge density than 30% and 10% (Fig. 4b2).

The measured hydrodynamic mean diameter from DLS is plotted against CPAM charge densities and dosages (Fig. 5). For 0.1 mg CPAM/m^2 dosage, the mean hydrodynamic diameter is 79 ± 5 nm and identical for CPAM of all charge densities. Similarly, for 0.5 mg CPAM/m^2 dosage, the hydrodynamic diameter increases to 150 ± 12 nm and remains independent of CPAM charge density. However, at the higher CPAM dosage of 1 mg CPAM/m^2 and at 10% and 30% charge density CPAM, the hydrodynamic diameter increases to 200 ± 20 nm, but further rises to 380 ± 30 nm with the 50% charge density CPAM.

4. Discussion

The zeta potential measured for SiO_2 NPs is −30 mV and that of cellulose is −26 mV [19]. Both SiO_2 NPs and cellulose are negatively and sufficiently charged to induce a strong electrostatic repulsion preventing significant SiO_2 NPs retention into the fibrous network. High retention of SiO_2 NPs requires a positively charged retention aid such as a high molecular weight polyelectrolyte to adsorb and aggregate NPs into the cellulose network.

Cationic-polyacrylamide (CPAM) is an efficient and widely used flocculant, well known as retention aid in the pulp and paper industry [31]. The CPAMs selected are positively charged

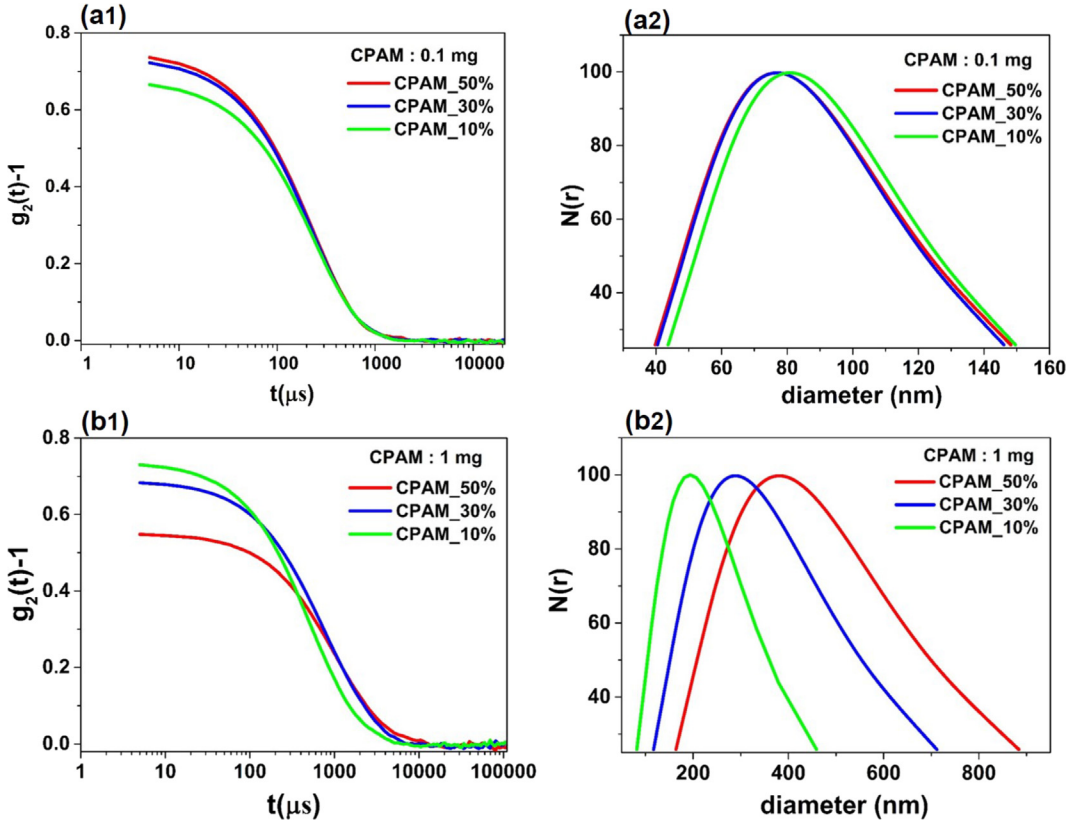

Fig. 4. (a1) DLS Correlation curves for SiO_2 NPs suspensions with CPAM of varying charge density of 50%, 30% and 10% at a fixed CPAM dosage of 0.1 mg CPAM/m^2 and (b1) 1.0 mg CPAM/m^2. The measured size distributions are given in (a2) and (b2), respectively.

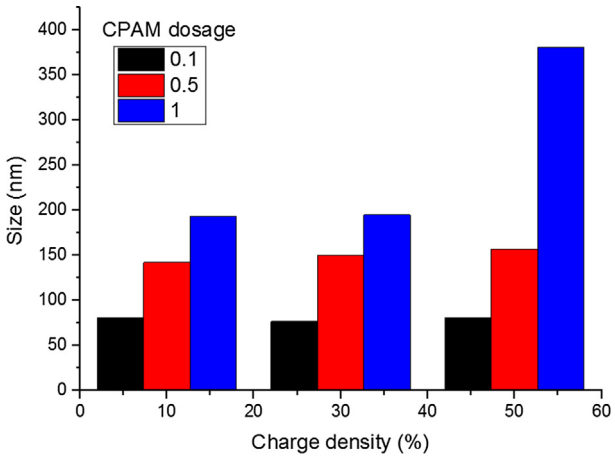

Fig. 5. Hydrodynamic SiO_2 NPs size measured from DLS for different CPAM dosages between 0.1 and 1.0 mg CPAM/m^2 and plotted against varying CPAM charge density between 10 and 50%.

polyelectrolytes having a very high molecular weight of 13 MDa corresponding to a radius of gyration (Rg) ranging between 30 and 40 nm [32]. The zeta potential of CPAM stabilized colloids ranges from +50 mV to +80 mV depending on charge density.

CPAMs of three different charge densities (20, 30 and 40%) were investigated at three different dosages (0.1, 0.5 and1.0 mg CPAM/m^2) to construct cellulose/SiO_2 NPs composites of well-defined structures. The amount of cellulose fibre was kept constant (1.2 mg) in all composites while NP concentration varied as a function of retention.

While preparing SiO_2/cellulose composites, CPAM was first mixed with the SiO_2 NPs. The diameter of SiO_2 NPs in suspension is around twice larger than the CPAM Rg. Sections of CPAM adsorb at the NP surface, driven by electrostatic attraction forces. The CPAM/SiO_2 suspension is then mixed with a stable cellulose suspension and the CPAM/SiO_2 entities adsorb onto and disperse within cellulose fibres network.

4.1. Effect of CPAM concentration

SAXS measurements (Fig. 2a2, b2, c2) show the scattering intensity of composites increases with CPAM dosage at a given polymer charge density. Increase in scattering intensity indicates higher retention of NPs in the cellulose network with high CPAM dosages. These results are consistent with the previously reported SAXS investigations on CPAM dosage effect on 8 and 22 nm SiO_2 NPs dispersion in the cellulose matrix [19,33]. A variation in the scattering intensity difference indicates the surface coverage is approaching the saturation plateau towards the high CPAM dosages. However, the scattering peaks position remains at the same q values revealing the NPs are surrounded by the same type of NPs forming a structure assembly with fixed inter-NPs distance. This constant inter-NP distance is reflected by the structure factor evaluated in Fig. 3b.

At low dosage (0.1 mg CPAM/m^2), the CPAM chain concentration in solution is limited and the SiO_2 NPs surface area available is sufficiently large to adsorb all CPAM. The CPAM chains adsorb into a flat conformation (trains) driven by a high electrostatic affinity for SiO_2 surface. The polymer chain distributes over the NP interface via multiple contacts (anchor points) resulting in a thin and permeable CPAM shell 2.5 nm thick. The adsorbed CPAM chain also bridges the nearby bare SiO_2 NPs (Fig. 6). NPs bridging leads to the formation of NPs assemblies of constant inter-NPs distance driven by the force balance between SiO_2-SiO_2 repulsion with CPAM-SiO_2 attraction (via bridging). At low CPAM dosage, fewer NPs

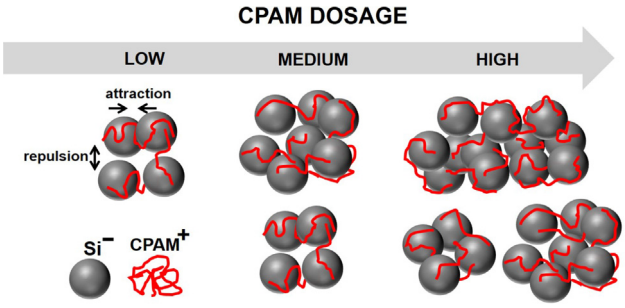

Fig. 6. Schematic on the effect of CPAM dosage (at a constant CPAM charge density) on the SiO_2 nanoparticles assembly.

assemblies are formed and most of the bare SiO_2 NPs remain stable in the suspension. The obtained adsorbed CPAM conformation thickness (2.5 nm) on SiO_2 NPs is in agreement with the previous reported adsorbed CPAM thickness (1.5 nm) on silicon wafers obtained by neutron reflectivity studies [32].

Increasing the CPAM dosage to 0.5 mg and 1.0 mg CPAM/m^2 increases the CPAM chains concentration in the suspension. The increased number of CPAM chains bridges additional bare SiO_2 NPs which creates newer assemblies of constant inter NPs distances (Fig. 6). This is in agreement with the DLS results (Fig. 5) showing the formation of NP dimers at 0.5 mg CPAM/m^2 and trimers and larger assemblies with 1.0 mg CPAM/m^2. The inclusion of NPs into bigger and new assemblies increases the NPs volume fractions [34] in the cellulose composite. The force balance between SiO_2-SiO_2 repulsion and CPAM-SiO_2 attraction dominates and insures a constant inter-NPs distance for all CPAM dosages.

4.2. Effect of CPAM charge

The absence of change in the shape and intensity of the SAXS curves (Fig. a1, b1, c1) indicates the inter-NPs interactions are unaffected by CPAM charge – at a particular dosage. The CPAM charge density (Table 1) is higher than the SiO_2 charge density (1.8×10^{-4} eq/g). The charge density of 50% CPAM is 7 times higher than that of SiO_2 NPs and twice as high as 10% CPAM. The average end to end chain length of the high charge density CPAM is expected to be higher than the low charge density polymers due to the stronger inter monomer repulsions.

Longer CPAM chains develop more contact points with the NP surface and better distribute to cover a larger area on single NPs. The CPAM chain also bridges the nearest SiO_2 NPs having a bare or partially CPAM covered surface. The force balance resulting from the SiO_2-SiO_2 repulsion with the SiO_2-CPAM attraction maintains the constant inter NPs distance observed. Interestingly, increase in CPAM charge density does not create significantly larger NPs assemblies so the NP volume fraction remains constant (Fig. a1, b1, c1).

Increasing the number of CPAM chains (dosage) in suspension has a significant effect on the NPs assembly formation. High CPAM dosage creates more NPs assemblies of high volume fraction which retain better in the cellulose fibrous network. However, increasing CPAM charge density (which increases chain length) at a particular CPAM dosage has no effect on the formed NPs assemblies and the inter-NPs interactions remains constant as unaffected.

4.3. CPAM/SiO_2 and cellulose fibre interactions

Upon mixing the CPAM/SiO_2 suspension with the cellulose fibres suspension, the CPAM covered NPs and their assemblies are electrostatically attracted towards the cellulose fibres; this NPs system adsorbs and retains onto the cellulose matrix. Low

CPAM dosage creates less and smaller NPs assemblies; this results in a lower NPs retention into the cellulose network. Increasing CPAM dosage increases the formation of newer and bigger NPs assemblies for a higher volume fraction of NPs retained in the cellulose fibre network. Adsorption at the cellulose interface also hinders the movements of SiO_2 assemblies and contributes to retaining the order/assembly structure of NPs.

5. Conclusion

We previously reported on the conformation of CPAM adsorbed on SiO_2 NPs of different sizes and its effect on the dispersion of the NPs in micro fibrillated cellulose (MFC) networks [29]. The CPAM chain interacts differently with different diameter of NPs which affects the composite nanostructures. CPAM dosage influences the NPs assembly within the CPAM chain which increases NPs volume fraction in the composites [19,33].

Here, the effect of dosage and charge density of very high molecular weight (13 MDa) cationic polyacrylamides (CPAM) on the formation and dispersion of SiO_2 NPs assemblies in cellulose nanofibre networks was investigated. A characterization methodology combining SAXS, DLS and SEM was developed. CPAMs are well known to adsorb onto many colloids to control their stability based on dosage, molecular weight and charge [4,15,18,21,24]. The radii of gyration of the CPAM investigated (30–40 nm) are half the average diameter of the SiO_2 NPs (74 nm). CPAM assembles NPs into cellulose fibre networks by a bridging mechanism. SAXS and DLS analysis show that increasing the CPAM dosage increases the average number of NPs in assemblies, which results in a higher retention of NPs in the cellulose network. However, increase in the CPAM charge density at a particular CPAM dosage has no effect on the assembly retention. Within the assembly, the NP-NP interdistance remains constant at 5 nm; this inter-NPs distance is affected neither by the CPAM dosage nor by its charge density. This is explained by the force balance arising from the electrostatic interactions between SiO_2 NPs and CPAM. The analytical methodology developed can be used to quantify the structure of any inorganic and metal NP of size 1–75 nm dispersed into composites with an organic continuous phase.

This work contributes to the manufacturing of functional biodegradable cellulose composites, and provides new analytical tools to gain a fundamental understanding of composites structures at the nanoscale.

Acknowledgment

Financial support is from Australian Research Council (ARC), Australian paper, Carter Holt Harvey, Circa, Norske Skog, Orora and Visy through the Industry Transformation Research Hub grant IH130100016. Many thanks to AquaTech for providing the CPAM polymers.

Appendix A. Supplementary material

Supplementary data associated with this article can be found, in the online version, at https://doi.org/10.1016/j.jcis.2018.06.009.

References

[1] M.A. Hubbe, A. Ferrer, P. Tyagi, Y.Y. Yin, C. Salas, L. Pal, O.J. Rojas, Bioresources 12 (2017) 2143.
[2] K.J. De France, T. Hoare, E.D. Cranston, Chem. Mater. 29 (2017) 4609.
[3] M. Ul-Islam, M.W. Ullah, S. Khan, T. Kamal, S. Ul-Islam, N. Shah, J.K. Park, Recent Pat. Nanotech. 10 (2016) 169.
[4] W.K.J. Mosse, D.V. Boger, G.P. Simon, G. Garnier, Langmuir 28 (2012) 3641.
[5] V. Pryamitsyn, V. Ganesan, Macromolecules 47 (2014) 6095.
[6] F.W. Wiegel, J. Phys. A: Math. Gen. 10 (1977) 299.
[7] J.-M.Y. Carrillo, A.V. Dobrynin, Langmuir 23 (2007) 2472.
[8] M. Turesson, C. Labbez, A. Nonat, Langmuir 27 (2011) 13572.
[9] F.T. Hesselink, J. Colloid Interface Sci. 60 (1977) 448.
[10] D.L. Elbert, C.B. Herbert, J.A. Hubbell, Langmuir 15 (1999) 5355.
[11] S.-C. Liufu, H.-N. Xiao, Y.-P. Li, J. Colloid Interface Sci. 285 (2005) 33.
[12] L.-E. Enarsson, L. Wågberg, J. Colloid Interface Sci. 325 (2008) 84.
[13] G. Yilmaz, T. Ellingham, L.S. Turng, Polym.-Basel 10 (2018).
[14] R.N. Carmean, T.E. Becker, M.B. Sims, B.S. Sumerlin, Chem.-Us 2 (2017) 93.
[15] Y.H. Ngo, D. Li, G.P. Simon, G. Garnier, Langmuir 28 (2012) 8782.
[16] M. Cadotte, M.-E. Tellier, A. Blanco, E. Fuente, T.G.M. van de Ven, P. Paris, Can. J. Chem. Eng. 85 (2007) 240.
[17] H. Zou, S.S. Wu, J. Shen, Chem. Rev. 108 (2008) 3893.
[18] D.H. Yoon, J.W. Jang, I.W. Cheong, Colloid Surf. A 411 (2012) 18.
[19] U.M. Garusinghe, V.S. Raghuwanshi, C.J. Garvey, S. Varanasi, C.R. Hutchinson, W. Batchelor, G. Garnier, Colloid Surf. A 513 (2017) 373.
[20] J. Zhou, F.W. Liu, C.Y. Pan, Plos One 9 (2014).
[21] J. Salmi, T. Nypelo, M. Osterberg, J. Laine, Bioresources 4 (2009) 602.
[22] Y.H. Ngo, D. Li, G.P. Simon, G. Garnier, J. Colloid Interface Sci. 392 (2013) 237.
[23] Y.H. Ngo, D. Li, G.P. Simon, G. Garnier, J. Colloid Interface Sci. 405 (2013) 71.
[24] D. Solberg, L. Wagberg, Colloid Surf. A 219 (2003) 161.
[25] V.S. Raghuwanshi, M. Ochmann, F. Polzer, A. Hoell, K. Rademann, Chem. Commun. 50 (2014) 8693.
[26] V.S. Raghuwanshi, M. Ochmann, A. Hoell, F. Polzer, K. Rademann, Langmuir 30 (2014) 6038.
[27] N.M. Kirby, S.T. Mudie, A.M. Hawley, D.J. Cookson, H.D.T. Mertens, N. Cowieson, V. Samardzic-Boban, J. Appl. Crystallogr. 46 (2013) 1670.
[28] O. Glatter, O. Kratky, Small-Angle X-ray Scattering, Academic Press, New York, 1982.
[29] V.S. Raghuwanshi, U.M. Garusinghe, J. Ilaysky, W.J. Batchelor, G. Gamier, J. Colloid Interface Sci. 510 (2018) 190.
[30] B.J. Berne, R. Pecora, Dynamic Light Scattering, Courier Dover Publications, New York, 2000.
[31] S.S. Wong, T.T. Teng, A.L. Ahmad, A. Zuhairi, G. Najafpour, J. Hazard. Mater. 135 (2006) 378.
[32] J.L. Su, C.J. Garvey, S. Holt, R.F. Tabor, B. Winther-Jensen, W. Batchelor, G. Garnier, J. Colloid Interface Sci. 448 (2015) 88.
[33] U. Garusinghe, V.S. Raghuwanshi, P. Raj, G. Garnier, W. Batchelor, 16TH Fundamental Research Symposium Advances in Pulp and Paper Research 2 (2017) 823.
[34] T. Cosgrove, P.C. Griffiths, P.M. Lloyd, Langmuir 11 (1995) 1457.